future pharmacology

MDPI

Article

Water-Soluble Cu(II) Complexes with Polypyridyl Ligands: Anticancer Activity and DNA Interaction

Herisson F. dos Santos [1,†], Nádija N. P. da Silva [1,†], George B. S. Pereira [1], Mauro A. Lima [1], Nailton M. Nascimento-Júnior [2], Renan L. de Farias [3], Amos O. Akinyemi [4] and Fillipe V. Rocha [1,*]

[1] Department of Chemistry, Federal University of São Carlos–UFSCar, São Carlos 13561-901, SP, Brazil; nadijasilva.nn@gmail.com (N.N.P.d.S.); george_bsp@hotmail.com (G.B.S.P.)
[2] Institute of Chemistry–Unesp, São Paulo State University (UNESP), Araraquara 14800-900, SP, Brazil; nailton.monteiro@unesp.br
[3] Department of Chemistry of Pontifícia Universidade Católica do Rio de Janeiro-PUC-Rio, Rio de Janeiro 22451-900, RJ, Brazil; renan.farias@puc-rio.br
[4] Department of Toxicology and Cancer Biology, College of Medicine, University of Kentucky, Lexington, KY 40536, USA; amos.olalekan7@uky.edu
* Correspondence: fillipevrocha@gmail.com
† These authors contributed equally to this work.

Abstract: Background/Objectives: Cu(II) complexes with polypyridine ligands have shown carcinogenic activity already described in the literature and appear as a possible alternative to cisplatin, which has several side effects. In view of this, four Cu(II) complexes with the formulas $[Cu(L1)(H_2O)_2](PF_6)_2$ (A1) and $[Cu(L2)(H_2O)_2](PF_6)_2$ (A2), $[Cu(L1)(bipy)](PF_6)_2$ (B1) and $[Cu(L2)(bipy)](PF_6)_2$ (B2) were synthesized, where L1 = dipyrido[1,2,5]oxadiazolo[3,4-b]quinoxaline, L2 = 6,7-dicyanodipyrido[2,2-d:2,3-f]quinoxaline, and bipy = 2,2′-bipyridine. **Methods:** The proposed structures supported characterization techniques (molar conductivity, elemental analyses, absorption spectroscopy in the infrared region, and UV–vis). The interaction of the complexes with DNA was evaluated through an ethidium bromide displacement assay, complemented by theoretical studies using molecular docking. Additionally, the cytotoxic activity of the complexes was tested against DU 145 (prostate tumor), MCF-7 (breast tumor), and PNT-2 (non-tumor prostate) cell lines, with all complexes showing promising results. **Results:** Among them, complex B1 exhibited the highest number of DNA contacts in molecular docking studies, a binding constant of 3.7×10^6 in the ethidium bromide displacement assay. It was the most selective complex (IS = 5.43) for the DU 145 (prostate tumor) cell line, demonstrating greater selectivity than cisplatin. **Conclusions:** This study has demonstrated the potential of the Cu(II) complexes obtained, which could be an alternative to platinum complexes in the future

Keywords: copper complexes; solubility; molecular docking; cancer

Academic Editor: Ali Zarrabi

Received: 23 January 2025
Revised: 13 February 2025
Accepted: 14 February 2025
Published: 19 February 2025

Citation: dos Santos, H.F.; da Silva, N.N.P.; Pereira, G.B.S.; Lima, M.A.; Nascimento-Júnior, N.M.; de Farias, R.L.; Akinyemi, A.O.; Rocha, F.V. Water-Soluble Cu(II) Complexes with Polypyridyl Ligands: Anticancer Activity and DNA Interaction. *Future Pharmacol.* **2025**, *5*, 10. https://doi.org/10.3390/futurepharmacol5010010

1. Introduction

Among the most abundant essential metals in organisms, copper (Cu) ranks third [1]. This trace element is involved in vital processes in humans, including cellular energy metabolism, iron absorption, and detoxification of reactive oxygen species (ROS) [2,3].

The coordination chemistry of copper varies with its oxidation state: the Cu(I) cation prefers sulfur-donating groups, whereas the Cu(II) cation favors oxygen- and nitrogen-donating groups [1]. This allows for optimal interactions with polypyridine ligands, such as phenanthroline and bipyridine. Specifically, the chemistry of Cu(II) is rich and versatile,

and its complexes have been studied for applications as anticancer agents, DNA structural probes, and biomolecule cleavage agents [4].

Copper, a d-block transition metal, and complexes with these metals have emerged as a potential alternative to cisplatin and its analogs for cancer treatment due to limitations associated with these compounds, such as severe side effects and drug resistance [5]. And copper complexes, because they have an endogenous and biocompatible metal in the coordination sphere, have fewer adverse effects and show cytotoxic activity against various tumor cells [6]. Nurmamat et al. (2021) synthesized a new copper complex [CuL(phen)(CH_3OH)][CuL(phen)]-CH_3CH_2OH-CH_3OH (P-FAH-Cu-phen) that inhibited the growth of BEL-7404 and H22 cells, with IC_{50} values (1.175 μg/mL and 1.097 μg/mL) much lower than those obtained for cisplatin (23.32 μg/mL and 27.5 μg/mL) [7]. The [Cu(II)$(SPy)_2Cl_2$] complex showed in vivo antitumor activity against EAC-induced ascites tumor and DLA-induced tumor in mice [8].

Studies with Cu(II) complexes and polypyridine ligands have already been reported, such as [Cu(sdmx-)2(phen)] which showed cytotoxic activity in breast cancer lines (MDA-MB-231 and MCF7), inhibited colony formation, and altered the morphology of cancer cells [9]. Bollu et al. (2019) also synthesized a series of complexes with polypyridine ligands that showed DNA intercalating capacity, anticancer and metastatic activity, induction of ROS, and apoptosis [10].

In the context of the global cancer burden—19.3 million new cases and an estimated 10 million deaths in 2020—the drawbacks of Pt(II) complexes [11,12], and our interest in developing new coordination complexes to overcome these limitations, of the carcinogenic activity of Cu(II) complexes with ligands already reported in the literature, we synthesized four novel Cu(II) complexes with polypyridine ligands. We evaluated their cytotoxic activity against DU 145 (prostate cancer), MCF-7 (breast cancer), and PNT-2 (non-cancerous prostate) cell lines. We also studied the interactions with DNA using the ethidium bromide assay and molecular docking.

2. Materials and Methods

2.1. General Methods

Infrared spectra were obtained using CsI pellets on a FTIR spectrometer (SHIMADZU IRTracer-1000. Data acquisition involved 42 scans per sample. UV–visible spectra were recorded in DMSO solutions using an UV-vis spectrophotometer (SHIMADZU UV-1650PC, Kyoto, Japan). The molar conductivity of the complexes was measured using a conductivity meter (Marconi, MA 521, Piracicaba, São Paulo, Brazil). Solutions with concentrations of 1×10^{-3} M were prepared in acetonitrile. The elemental analysis of the complexes was carried out on a Fisions CHNS analyzer model EA 1108 from the Analytical Center of the Chemistry Department of the Federal University of São Carlos, São Carlos, São Paulo, Brazil.

2.2. Synthesis of Ligands L1 and L2

The ligands L1 (8a,13b-dihydro-[1,2,5]oxadiazolo[3′,4′:5,6]pyrazino[2,3-f][1,10]phenanthroline) and L2 (2,3,4b,12a-tetrahydropyrazino [2,3-f][1,10]phenanthroline-2,3-dicarbonitrile) were synthesized following the methodology described in the literature [13].

2.3. Synthesis of Complex [Cu(L1)$(H_2O)_2$]$(PF_6)_2$ (A1) and [Cu(L2)$(H_2O)_2$]$(PF_6)_2$ (A2)

In a 250 mL round-bottom flask, 100 mg of $CuSO_4 \cdot 5H_2O$ was dissolved in 50 mL water. To this solution, a suspension of ligand L1 (110 mg in 50 mL of ethanol) for A1 or ligand L2 (113.5 mg in 50 mL of ethanol) for A2 was added dropwise. The resulting solution was refluxed at 90 °C for 24 h. After this period, the volume was reduced, and

precipitation was induced by immersion in an ice bath. A green solid was obtained, filtered, and recrystallized in hot water with excess NH_4PF_6. The solid was washed with water at room temperature and dried under vacuum. A1: Yield: 60%. Elemental analysis calculated for $C_{14}H_{10}CuF_{12}N_6O_3P_2$: C, 23.33%; H, 1.52%; N, 12.66%. Experimental: C, 24.50%; H, 1.70%; N, 12.09%. Molar conductivity in acetonitrile: 235 $S{\cdot}cm^{-2}{\cdot}mol^{-1}$. Selected IR (CsI; cm^{-1}): 3084 (νH-C=); 1600–1400 (νC=C); 841 (νP-F); 559 (δP-F). A2: Yield: 60%. Elemental analysis calculated for $C_{16}H_{12}CuF_{12}N_6O_2P_2$: C, 28.61%; H, 1.50%; N, 12.51%. Experimental: C, 27.73%; H, 1.83%; N, 11.45%. Molar conductivity in acetonitrile: 248 $S{\cdot}cm^{-2}{\cdot}mol^{-1}$. Selected IR (CsI; cm^{-1}): 3089 (νH-C=); 1600–1400 (νC=C); 2235 (νC≡N); 841 (νP-F); 559 (δP-F).

2.4. Synthesis of Complex [Cu(L1)(bipy)](PF$_6$)$_2$ (B1) and [Cu(L2)(bipy)](PF$_6$)$_2$ (B2)

In a 100 mL round-bottom flask, 100 mg of complex A1 (for B1) or A2 (for B2) was dissolved in 50 mL of acetone. To this solution, 25 mg of 2,2′-bipyridine (bipy) was added. The volume was reduced, and precipitation was induced by immersion in an ice bath, forming a brown solid. The solid was filtered, washed with cold ethanol, and dried under a vacuum. B1: Yield: 50%. Elemental analysis calculated for $C_{27}H_{20}CuF_{12}N_8O_2P_2$: C, 38.52%; H, 2.39%; N, 13.31%. Experimental: C, 37.92%; H, 2.50%; N, 13.10%. Molar conductivity in acetonitrile: 146 $S{\cdot}cm^{-2}{\cdot}mol^{-1}$. Selected IR (CsI; cm^{-1}): 3091 (νH-C=); 1600–1400 (νC=C); 841 (νP-F); 559 (δP-F). B2: Yield: 50%. Elemental analysis calculated for $C_{29}H_{22}CuF_{12}N_8OP_2$: C, 40.88%; H, 2.60%; N, 13.15%. Experimental: C, 40.35%; H, 3.02%; N, 12.77%. Molar conductivity in acetonitrile: 177 $S{\cdot}cm^{-2}{\cdot}mol^{-1}$. Selected IR (CsI; cm^{-1}): 3083 (νH-C=); 1600–1400 (νC=C); 2238 (νC≡N); 841 (νP-F); 559 (δP-F).

2.5. Molecular Docking

The three-dimensional coordinates of the target biomolecule were obtained from the Protein Data Bank (PDB ID: 1G3X) [14], whose structure was resolved by X-ray diffraction at a resolution of 2.7 Å. Before conducting molecular docking calculations, hydrogen atoms were automatically added to the biomolecule, considering protonation states at pH 7.4. Subsequently, all water molecules and the co-crystallized ligand (acridine-9-carbaldehyde, 9AC) were removed. Redocking calculations were performed over 50 runs using the ChemPLP scoring function [15] within a rigid model available in the GOLD software (v 5.7) [16]. Using 9AC as a reference co-ligand, a radius of 10 Å was selected for the docking model. The Cu(II) complexes were docked as in the redocking process. The poses with the highest scores were extracted as solutions, and the results were visualized and interpreted using the graphical platforms Pymol [17] and DSV (v 17.2.0).

2.6. Cell Viability Assay

Cytotoxicity assays were performed using the following cell lines: DU 145 (prostate cancer), MCF-7 (breast cancer), and PNT-2 (non-tumor prostate). The cells were cultured in DMEM (Dulbecco Modified Eagle Medium) with 10% (*v*/*v*) FBS (fetal bovine serum) in plastic flasks Corning (Oneonta, NY, USA) and stored in an incubator at 37 °C with a 5% CO_2 atmosphere. Cell counting was performed using a Trypan Blue stain in a Neubauer chamber (Bio-Rad Laboratories, Hercules, CA, USA) under a Nikon Eclipse TS100 microscope (Nikon, Tokyo, Japan). After counting the cell suspension, aliquots of 150 µL containing 1.5×10^4 cells/mL were added to 96-well plates. The plates were kept in the incubator for 24 h, and then 0.75 µL of a DMSO solution (0.01%) containing the ligand or complexes was added to each well. The plates were incubated for an additional 48 h. After incubation, 50 µL of an MTT (3-(4,5-Dimethylthiazol-2-yl)-2,5-Diphenyl Tetrazolium Bromide) solution (1 mg/mL) was added to each well and incubated again for 4 h. After this period, the solution in each well was removed, and 100 µL of DMSO was added.

Absorbance measurements were taken from each well using the BioTek hybrid microplate reader, model SYNERGY H1 (BioTek, Agilent, Santa Clara, CA, USA). The obtained data were processed using Excel 2010 and GraphPad Prism 5.01.

2.7. DNA Interaction Study Using Ethidium Bromide

An ethidium bromide solution was mixed with a CT-DNA (DeoxyriboNucleic Acid sodium salt from Calf Thymus) solution so that the final concentration of each species in the solution was 50 µM. This solution was titrated with the complex of interest at concentrations ranging from 0 to 50 µM. The result of this titration was monitored by the decrease in the emission intensity of the EB + DNA adduct curve as the complex was added.

3. Results

3.1. Synthesis and Characterization

The four complexes were synthesized from copper sulfate and the ligands L1 and L2 (Figure 1). They exhibited green or brown coloration and partial solubility in water. The techniques used to characterize the complexes supported the proposed structures.

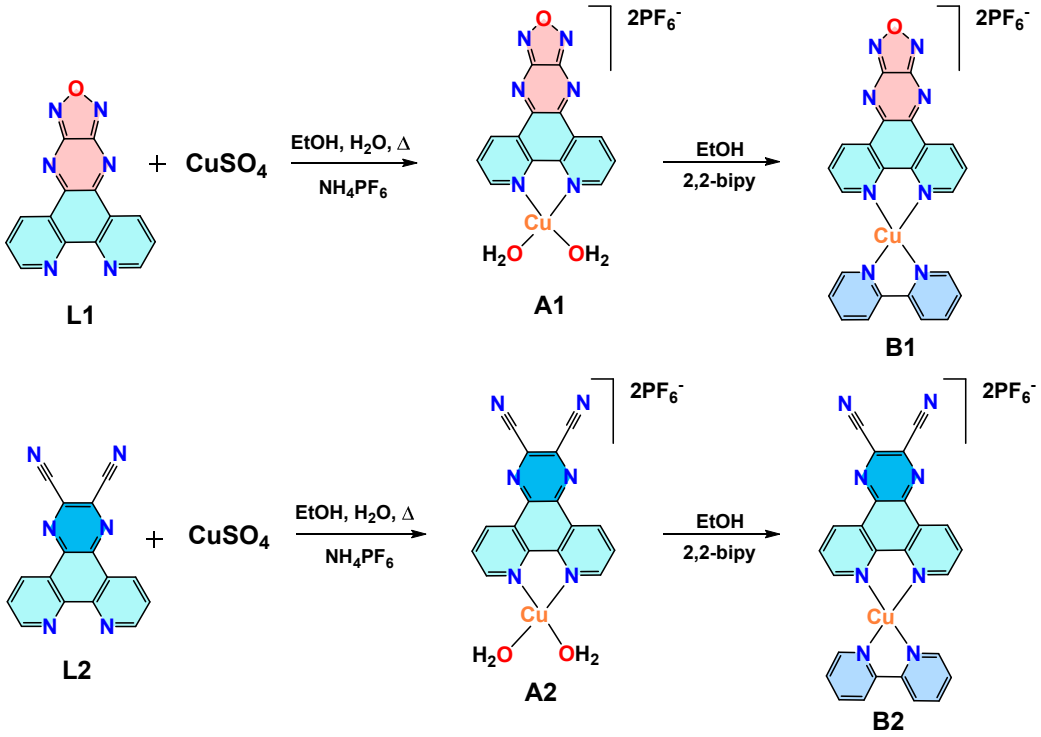

Figure 1. Synthetic route for the preparation of Cu(II) complexes.

The data obtained through the techniques used to characterize the complexes corroborated the proposed structures. The molar conductivity values in acetonitrile indicate that the complexes ($S \cdot cm^{-2} \cdot mol^{-1}$: A1: 235; A2: 248; B1: 146; B2: 177) are 2:1 electrolytes. The experimental carbon, nitrogen, and hydrogen percentages agree with the theoretical values. The infrared spectra show stretching of the νH-C= (3091–3083 cm^{-1}), νC≡N (2238–2235 cm^{-1}), and νC=C (1600–1400 cm^{-1}) bonds of the polypyridine ligands, stretching of the νP-F (841 cm^{-1}) bond, and angular deformation of the δP-F (559 cm^{-1}) bond of the PF_6^- ion (Figure 2).

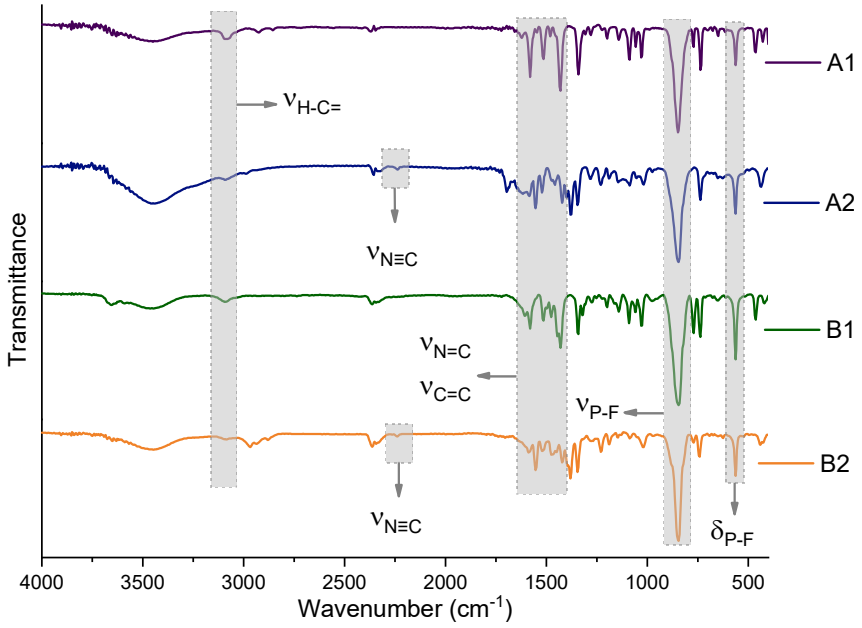

Figure 2. Infrared spectra of the synthesized complexes with the assignment of the leading bands.

3.2. Molecular Docking

The molecular modeling approaches employed in this study are based on classical mechanics, which considers atoms as hard spheres connected by springs. Using this technique, the geometric parameters and complementarity between the structures of the Cu(II) complexes (A1, A2, B1, and B2) and the DNA fragment d(CGCGAATTCGCG)2 were evaluated [14]. The crystalline structure of the DNA (B-form) includes the aromatic fragment acridine-9-carbaldehyde (9AC) as a reference intercalator. A redocking approach was applied to validate the computational methodology [18]. The native ligand was extracted from the interaction site and its original orientation was recalculated. As a validation criterion, the root mean square deviation (RMSD) between the experimental atomic coordinates and the modeled coordinates is expected to be less than 2.0 Å (Figure 3).

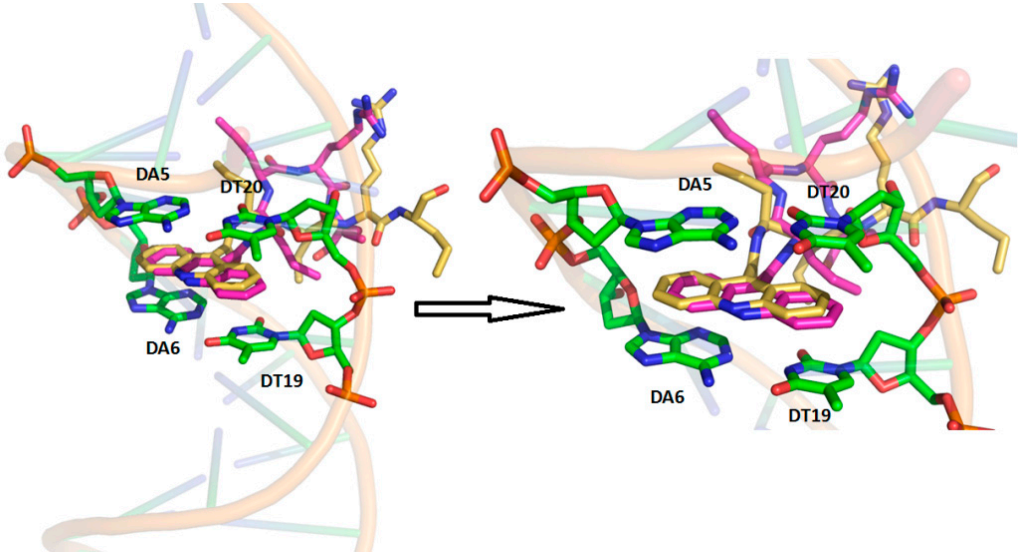

Figure 3. Docking pose of the co-crystallized ligand (carbons in magenta) and the adjacent nucleobases (DA5, DA6, DT19, and DT20) at the interaction site (carbons in green). Overlap of both aromatic fragments (theoretical and experimental). DA and DT represent deoxyadenosine and deoxythymidine, respectively.

Figure 3 illustrates the intercalative binding mode of the polycyclic aromatic fragment 9AC co-crystallized (carbons in yellow) and the overlaid computational model (carbons in magenta). The RMSD value was 0.6628 Å, indicating good agreement between the experimental and computational data. Subsequently, geometric parameters were evaluated for Cu(II) complexes containing ligands derived from dipyrido[3,2-a:2′,3′-c]phenazine in the AA-TT hydrophobic pocket (Figures 4 and 5).

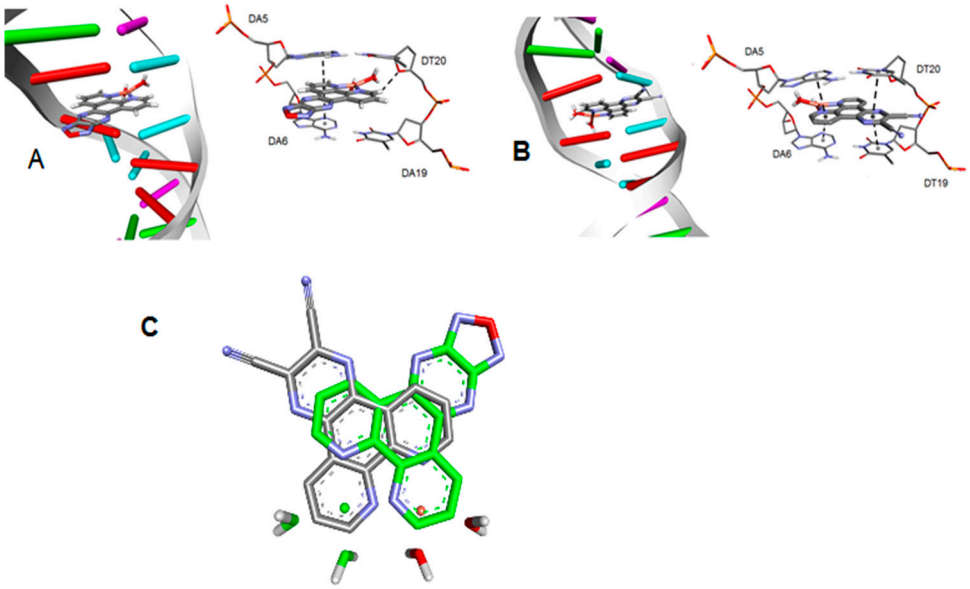

Figure 4. (**A**,**B**) Docking poses for A1 and A2 in the hydrophobic AA-TT pocket; (**C**) preferred ligand orientations based on modifications in the pyrazinic fragment.

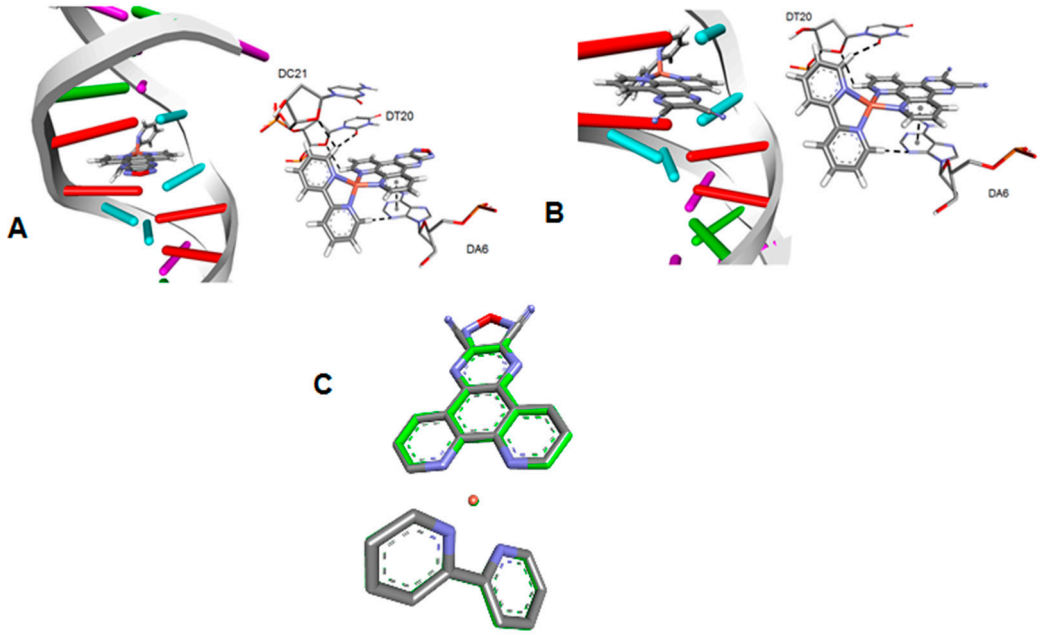

Figure 5. (**A**,**B**) docking poses for B1 and B2 in the AA-TT hydrophobic pocket. (**C**) Preferred orientations of the ligands, considering the modifications in the pyrazine fragment.

It can be inferred from the docking data that, between compounds A1 and A2, nitrile substituents in the pyrazinic fragment induce variations in the ligand's orientation within the binding site. As a result, molecular recognition via π–π stacking ($X_{vdw} \leq 3.4X$) [19] is more pronounced for compound A2 in the hydrophobic pocket compared to A1 (Figure 3).

Conversely, the substitutions on the pyrazinic fragment did not result in significant variations in the orientations of compounds B1 and B2 within the binding site. However, replacing the labile ligands with 2,2′-bipyridine increased the steric volume around the metal's coordination environment. Consequently, a reduced preference for intercalative interactions is observed compared to the aqua complexes (Figure 5).

It is essential to highlight that from the sp^2 hybridization of the C-H groups in 2,2′-bipyridine, the formation of non-classical hydrogen bonds (C-H···O) with the O-acceptor atoms of the proximal riboses is observed (as a criterion, X_{vdW} between H and O $\leq$ 2.72 Å) [20], as shown in Figures 6 and 7.

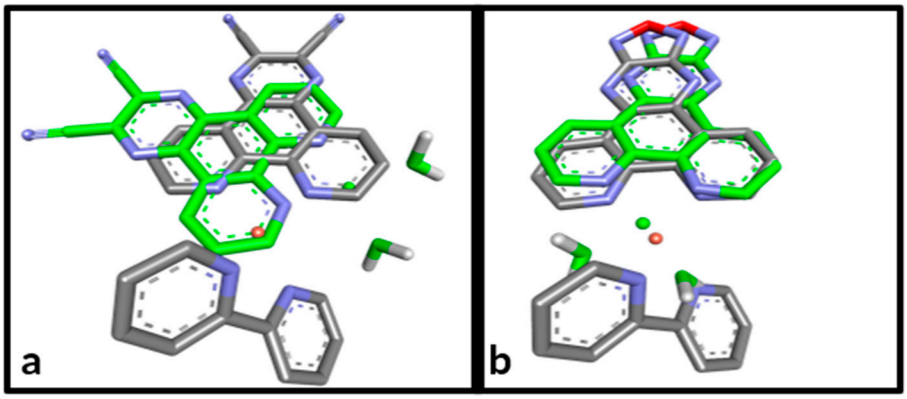

Figure 6. Docking poses show the relative orientations of complexes A2 and B2 (**a**) and A1 and B1 (**b**) within the binding site.

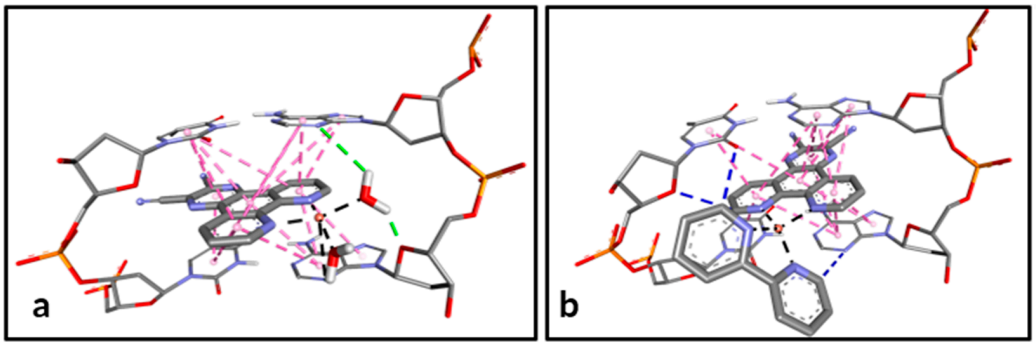

Figure 7. DNA interaction points of the A2 (**a**) and B2 (**b**) complexes were calculated by molecular docking with water molecules omitted.

Therefore, based on the best scoring values for the docking poses (Table 1), it can be deduced that the presence of nitrile substituents and the bipyridine ligand directly influence the affinity of these compounds for the DNA biomolecule. Furthermore, the optimal number of intermolecular contacts with DNA was found to be four for the compounds in question.

Table 1. Score, type, and total intermolecular contacts were observed for molecular docking calculations.

Complex	Score	sp^2 C-H···O	π–π	Total Contacts
A1	70.75	1	2	3
A2	77.85	0	4	4
B1	75.68	4	1	5
B2	77.61	3	1	4

3.3. Cytotoxicity Assay

The cytotoxicity of the complexes was evaluated in the DU 145 (prostate cancer), MCF-7 (breast cancer), and PNT-2 (non-cancerous prostate) cell lines. All complexes exhibited significant reductions in cytotoxicity when compared to their respective ligands (Table 2), indicating a synergistic action between the already biologically active organic ligands and the metal centers. The complexes with the L1 ligand were more active than those containing L2, consistent with the behavior observed for the free ligands. In the DU 145 cell line, the complexes derived from the L1 ligand were at least seven times more active than those with the L2 ligand; in the MCF-7 cell line, this difference reached tenfold.

Table 2. IC_{50} (μM) results obtained after 24 h of incubation for the ligands (L1, L2), the complexes (A1, A2, B1, B2), and cisplatin in different cell lines.

	DU 145	MCF-7	PNT-2	SI *	SI **
L1	3.12 ± 0.06	1.44 ± 0.15	1.59 ± 0.06	0.51	1.10
L2	5.83 ± 0.26	23.26 ± 0.85	8.67 ± 0.10	1.48	0.37
A1	0.32 ± 0.03	0.40 ± 0.02	0.49 ± 0.06	1.53	1.22
A2	2.36 ± 0.05	4.52 ± 0.37	9.15 ± 0.54	3.87	2.02
B1	0.37 ± 0.04	0.47 ± 0.01	2.01 ± 0.05	5.43	4.27
B2	3.66 ± 0.91	4.33 ± 0.15	5.51 ± 0.34	1.50	1.27
Cisplatin	15.0 ± 1.40	19.90 ± 4.20	11.74 ± 1.20	0.78	0.59

* SI: (PNT-2/DU 145); ** SI: (PNT-2/MCF-7).

The B1 complex was the most selective in both tumor cell lines compared to the non-tumor cell line, demonstrating greater selectivity than cisplatin, the reference drug. In molecular docking, the B1 complex showed more interactions with DNA. Therefore, an experimental displacement assay with ethidium bromide was performed to assess potential DNA intercalation. It was observed that the complex suppresses the fluorescence of the DNA-ethidium bromide adduct (Figure 8), indicating a possible intercalation, as ethidium bromide is an intercalating agent. Using the Stern–Volmer equation, the DNA-complex interaction constant was determined to be 3.7×10^6, of the same magnitude as Acridine [21], a standard intercalator.

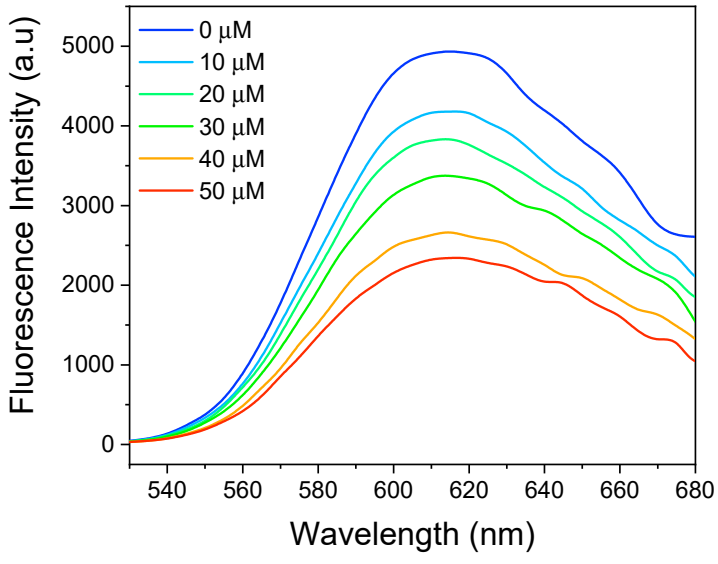

Figure 8. Variation in the emission intensity of the CT-DNA + ethidium bromide adducts with the addition of the complex.

4. Discussion

The Cu(II) ion was chosen due to its economic advantages, planar geometry, and d9 electronic configuration, which allows charge transfer in the visible spectrum when combined with the appropriate ligand. Moreover, Cu(II)-containing compounds are already well-known in the literature for their promising anticancer activity [22,23].

Polypyridine ligands, such as phenanthroline and bipyridine, have been extensively studied because they impart rigidity and thermodynamic stability to the complex when coordinated in a bidentate manner [24], facilitating hydrophobic interactions in the biological medium. Their structure, with π-type empty orbitals, enables electronic movements in the visible region when combined with electron-rich d-atoms [24,25].

The combination of the metal center and the polypyridine ligands formed complexes partially soluble in water, which allowed the cytotoxicity tests to be carried out using 99.99% water and only 0.01% DMSO. It is important to highlight this characteristic of the compounds, as the fac-[$RuIIICl_3(NH_3)_3$] complex was previously considered unsuitable for further clinical evaluation due to its limited solubility in water [26].

The IC_{50} (concentration of the complex at which 50% of the cells are viable compared to the control) values obtained for the A1, A2, B1, and B2 complexes in the DU 145 (A1: 0.32 ± 0.03 μM; A2: 2.36 ± 0.05 μM; B1: 0.37 ± 0.04 μM; B2: 3.66 ± 0.91 μM) and MCF7 (A1: 0.40 ± 0.02 μM; A2: 4.52 ± 0.37 μM; B1: 0.47 ± 0.01 μM; B2: 4.33 ± 0. 15 μM) were generally lower than the values obtained for the ligands L1 (DU 145: 3.12 ± 0.06 μM; MCF7: 1.44 ± 0.15 μM) and L2 (DU 145: 5.83 ± 0.26 μM; MCF7: 23.26 ± 0.85 μM), showing that the final combination obtained by forming the complexes is beneficial in inhibiting the growth of tumor cells. The B1 complex showed an IC_{50} around 40 times lower than cisplatin in the DU 145 (15.0 ± 1.40 μM) and MCF-7 (19.90 ± 4.20 μM) lineages. This behavior was also observed by Carcelli et al. (2020) in copper complexes, where the complexation of ligands with the metal significantly enhanced the cytotoxic activity of the isolated ligands, and the formed complexes exhibited IC_{50} values much lower than cisplatin [27].

All the synthesized complexes in this study were more selective than cisplatin in the cell lines DU 145 (A1: 1.53; A2: 3.87; B1: 5.43; B2: 1.50; cisplatin: 0.78) and MCF-7 (A1: 1.22; A2: 2.02; B1: 4.47; B2: 1.27; cisplatin: 0.59). The selectivity index (SI), which represents how selective the compound is to tumor cells relative to normal cells, with a value of 2.0 or higher, is considered promising [28]. This behavior indicates that the obtained complexes cause less damage to normal cells than cisplatin in the cell lines used.

The study of DNA interactions is key to the development of new anticancer agents, as many effective chemotherapeutics act by targeting DNA, disrupting replication and transcription, and inducing cancer cell death. Understanding how metal-based complexes or novel ligands interact with DNA allows the design of more selective and potent drugs, minimizing side effects and overcoming resistance mechanisms. Thus, theoretical calculations through molecular docking were initially performed. Molecular modeling employs tools for constructing and analyzing complex systems computationally. The technique starts with an experimentally known receptor structure and adjusts the drug candidate to fit this site [15,29]. Interaction calculations allow comparisons between experimental and theoretical data, helping to conclude about a possible interaction with the system under study. According to molecular docking calculations, the complex that showed higher selectivity also exhibited the highest number of contacts with DNA. The interaction of the B1 complex with DNA was evaluated through an ethidium bromide displacement assay to verify the correlation between the theoretical and experimental studies. Since the ethidium bromide displacement experiment indicates intercalation into DNA [20], it is suggested that in the B1 complex the phenanthroline ligands intercalate between the nitrogenous bases of this biomolecule, as well as carrying out hydrophobic interactions, justifying the IC_{50}

values and the selectivity index. Studies have shown that copper complexes can interact covalently or non-covalently (intercalative, electrostatic, and interactions with the major or minor grooves) with DNA. DNA damage induced by these interactions may be linked to anticancer activity [30]. A study by Machado et al. (2021) [31] on copper complexes found that a Cu(II) complex with hydrazide of 4-fluorophenoxyacetic acid and phenanthroline exhibited anticancer activity in tumor cell lines, induced DNA damage, caused cell cycle arrest at the G0/G1 phase, and triggered apoptosis.

5. Conclusions

The Cu(II) compounds synthesized showed relative solubility in water, which allowed the cytotoxicity tests to be carried out using more than 99% water. All four complexes (A1, A2, B1, and B2) showed higher cytotoxicity when compared to their respective isolated ligands (L1 and L2), which highlights the importance of this metal center-polypyridine ligand combination in improving the cytotoxic activity of these ligands. The results obtained are promising, especially for the B1 complex, which showed the highest selectivity index in DU 145 (5.43) and MCF7 (4.27) tumor cells, even surpassing the selectivity of cisplatin in these same strains (DU 145: 0.78; MCF7: 0.59).

The experimental and theoretical studies on the interaction with DNA were important for understanding the alterations that the complexes promote in this biomolecule. At this point, the B1 complex also stands out for having a greater number of contacts with DNA and intercalative capacity using the ethidium bromide assay, which is a possible justification for its anticancer activity and selectivity.

This study demonstrated the potential of the Cu(II) complexes obtained, which could be an alternative to platinum complexes in the future. However, further studies aimed at investigating how these complexes act on cancer cells should be carried out.

Author Contributions: Conceptualization, H.F.d.S. and F.V.R.; methodology, H.F.d.S., R.L.d.F. and M.A.L.; investigation and validation, H.F.d.S., M.A.L. and N.M.N.-J.; writing—original draft preparation, N.N.P.d.S. and G.B.S.P.; writing—review and editing, N.N.P.d.S., G.B.S.P., A.O.A. and F.V.R. All authors have read and agreed to the published version of the manuscript.

Funding: This research was funded by the National Council for Scientific and Technological Development (CNPq-401681/2023-8), the Coordination for the Improvement of Higher Education Personnel (CAPES), FINEP (no. 01.22.0182), and the São Paulo State Research Foundation (FAPESP) (2019/11242-1, 2022/02876-0 and 2018/00187-7).

Institutional Review Board Statement: Not applicable.

Informed Consent Statement: Not applicable.

Data Availability Statement: Data are contained within the article.

Conflicts of Interest: The authors declare no conflicts of interest.

References

1. da Silva, D.A.; De Luca, A.; Squitti, R.; Rongioletti, M.; Rossi, L.; Machado, C.M.; Cerchiaro, G. Copper in tumors and the use of copper-based compounds in cancer treatment. *J. Inorg. Biochem.* **2022**, *226*, 111634. [CrossRef]
2. Guan, D.; Zhao, L.; Shi, X.; Ma, X.; Chen, Z. Copper in cancer: From pathogenesis to therapy. *Biomed. Pharmacother.* **2023**, *163*, 114791. [CrossRef] [PubMed]
3. Palmeira-Mello, M.V.; Caballero, A.B.; Lopez-Espinar, A.; Guedes, G.P.; Caubet, A.; de Souza, A.M.T.; Lanznaster, M.; Gamez, P. DNA-interacting properties of two analogous square-planar cis-chlorido complexes: Copper versus palladium. *JBIC J. Biol. Inorg. Chem.* **2021**, *26*, 727–740. [CrossRef] [PubMed]
4. Erxleben, A. Interactions of copper complexes with nucleic acids. *Coord. Chem. Rev.* **2018**, *360*, 92–121. [CrossRef]
5. Oliveira, C.; Oliveira, A.; Pelinski, L.; Cailliau, K. Complexos de cobre como agentes anticancerígenos direcionados às topoisomerases I e II. *Cânceres* **2020**, *12*, 2863.

6. Ghorbanpour, M.; Shayanfar, A.; Soltani, B. Copper pyrazole complexes as potential anticancer agents: Evaluation of cytotoxic response against cancer cells and their mechanistic action at the molecular level. *Coord. Chem. Rev.* **2024**, *498*, 215459. [CrossRef]
7. Nurmamat, M.; Yan, H.; Wang, R.; Zhao, H.; Li, Y.; Wang, X.; Nurmaimaiti, K.; Kurmanjiang, T.; Luo, D.; Baodi, J.; et al. Novel copper (II) complex with a 4-acylpyrazolone derivative and coligand induce apoptosis in liver cancer cells. *ACS Med. Chem. Lett.* **2021**, *12*, 467–476. [CrossRef] [PubMed]
8. Kumar, K.S.; Reena, V.N. Design, synthesis, crystal structure, antitumour and antimicrobial evaluation of a novel substituted pyrazole and its some metal complexes. *Mater. Today Proc.* **2022**, *62*, 5427–5433. [CrossRef]
9. Teles, R.H.G.; Graminha, A.E.; Rivera-Cruz, C.M.; Nakahata, D.H.; Formiga, A.L.B.; Corbi, P.P.; Figueiredo, M.L.; Cominetti, M.R. Copper transporter 1 affinity as a delivery strategy to improve the cytotoxic profile of rationally designed copper (II) complexes for cancer treatment. *Toxicol. Vitr.* **2020**, *67*, 104922. [CrossRef]
10. Bollu, V.S.; Bathini, T.; Barui, A.K.; Roy, A.; Ragi, N.C.; MalOth, S.; Sripadi, P.; Sreedhar, B.; Nagababu, P.; Patra, C.R. Design of DNA-intercalators based copper (II) complexes, investigation of their potential anti-cancer activity and sub-chronic toxicity. *Mater. Sci. Eng. C* **2019**, *105*, 110079. [CrossRef]
11. Masuri, S.; Vaňhara, P.; Cabiddu, M.G.; Moráň, L.; Havel, J.; Cadoni, E.; Pivetta, T. Copper (II) phenanthroline-based complexes as potential anticancer drugs: A walkthrough on the mechanisms of action. *Molecules* **2021**, *27*, 49. [CrossRef] [PubMed]
12. Sung, H.; Ferlay, J.; Oliveira, R.L.; Oliveira, M.; Soerjomataram, I.; Oliveira, A.; Bray, F. Estatísticas Globais do Câncer 2020: Estimativas GLOBOCAN de incidência e mortalidade em todo o mundo para 36 cânceres em 185 países. *CA Câncer J. Clin.* **2021**, *71*, 209–249. [CrossRef] [PubMed]
13. Rocha, J.S.; Pereira, G.B.S.; Oliveira, G.P.; Lima, M.A.; Araujo-neto, J.H.; Pinto, L.S.; Forim, M.R.; Zanetti, R.D.; Netto, A.V.G.; Castellano, E.E.; et al. Synthesis and characterization of silver(I) complexes bearing phenanthroline derivatives as ligands: Cytotoxicity and DNA interaction evaluation. *Inorg. Chem. Commun.* **2021**, *131*, 108757. [CrossRef]
14. Malinina, L.; Soler-López, M.; Aymamí, J.; Subirana, J.A. Intercalation of an Acridine—Peptide Drug in an AA/TT Base Step in the Crystal Structure of [d (CGCGAATTCGCG)] 2 with Six Duplexes and Seven Mg^{2+} Ions in the Asymmetric Unit. *Biochemistry* **2002**, *41*, 9341–9348. [CrossRef] [PubMed]
15. Waszkowycz, B. Towards improving compound selection in structure-based virtual screening. *Drug Discov. Today* **2008**, *13*, 219–226. [CrossRef] [PubMed]
16. Pagadala, N.S.; Syed, K.; Tuszynski, J. Software for molecular docking: A review. *Biophys. Rev.* **2017**, *9*, 91–102. [CrossRef] [PubMed]
17. Delano, W.L. *The PyMOL Molecular Graphics System*; DeLano Scientific: San Carlos, Venezuela, 2002.
18. Morris, G.M.; Huey, R.; Lindstrom, W.; Sanner, M.F.; Belew, R.K.; Goodsell, D.S.; Olson, A.J. AutoDock4 and AutoDockTools4: Automated docking with selective receptor flexibility. *J. Comput. Chem.* **2009**, *30*, 2785–2791. [CrossRef]
19. Rowland, R.S.; Taylor, R. Intermolecular nonbonded contact distances in organic crystal structures: Comparison with distances expected from van der Waals radii. *J. Phys. Chem.* **1996**, *100*, 7384–7391. [CrossRef]
20. Pinho, J.O.; da Silva, I.V.; Amaral, J.D.; Rodrigues, C.M.; Casini, A.; Soveral, G.; Gaspar, M.M. Therapeutic potential of a copper complex loaded in pH-sensitive long circulating liposomes for colon cancer management. *Int. J. Pharm.* **2021**, *599*, 120463. [CrossRef] [PubMed]
21. Nafisi, S.; Saboury, A.A.; Keramat, N.; Neault, J.; Tajmir-Riahi, H. Stability and structural features of DNA intercalation with ethidium bromide, acridine orange and methylene blue. *J. Mol. Struct.* **2007**, *827*, 35–43. [CrossRef]
22. Hussain, A.; AlAjmi, M.F.; Rehman, M.T.; Amir, S.; Husain, F.M.; Alsalme, A.; Siddiqui, M.A.; AlKhedhairy, A.A.; Khan, R.A. Copper (II) complexes as potential anticancer and Nonsteroidal anti-inflammatory agents: In vitro and in vivo studies. *Sci. Rep.* **2019**, *9*, 5237. [CrossRef]
23. Ballance, D.G.; Bryantsev, V.S.; Ivanov, A.S.; Dai, S.; Hancock, R.D. Complexation of Lanthanides and other metal ions by the polypyridyl ligand quaterpyridine: Relation between metal ion size, chelate ring size, and complex stability. *Inorganica Chim. Acta* **2019**, *488*, 19–27. [CrossRef]
24. Sergeeva, N.N.; Donnier-Marechal, M.; Vaz, G.M.; Davies, A.M.; Senge, M.O. Stability and spectral properties of europium and zinc phenanthroline complexes as luminescent probes in high content cell-imaging analysis. *J. Inorg. Biochem.* **2011**, *105*, 1589–1595. [CrossRef] [PubMed]
25. Hadadzadeh, H.; Mansouri, G.; Rezvani, A.; Khavasi, H.R.; Skelton, B.W.; Makha, M.; Charati, F.R. Mononuclear nickel (II) complexes coordinated by polypyridyl ligands. *Polyhedron* **2011**, *30*, 2535–2543. [CrossRef]
26. Katheria, S. Ruthenium complexes as potential cancer cell growth inhibitors for targeted chemotherapy. *ChemistrySelect* **2022**, *7*, e202201645. [CrossRef]
27. Carcelli, M.; Tegoni, M.; Bartoli, J.; Marzano, C.; Pelosi, G.; Salvalaio, M.; Rogolino, D.; Gandin, V. In vitro and in vivo anticancer activity of tridentate thiosemicarbazone copper complexes: Unravelling an unexplored pharmacological target. *Eur. J. Med. Chem.* **2020**, *194*, 112266. [CrossRef] [PubMed]

28. Suffness, M.; Pezzuto, J.M. Assays related to cancer drug discovery. In *Methods in Plant Biochemistry*; Hostettmann, K., Ed.; Academic Press: London, UK, 1991; pp. 71–133.
29. Chen, Y.-C. Beware of docking! *Trends Pharmacol. Sci.* **2015**, *36*, 78–95. [CrossRef] [PubMed]
30. Wang, Y.; Tang, T.; Yuan, Y.; Li, N.; Wang, X.; Guan, J. Copper and Copper Complexes in Tumor Therapy. *ChemMedChem* **2024**, *19*, e202400060. [CrossRef] [PubMed]
31. Machado, P.H.A.; Paixão, D.A.; Lino, R.C.; de Souza, T.R.; de Souza Bontempo, N.J.; Sousa, L.M.; Van Petten de Vasconcelos Azevedo, F.; Orsolin, P.C.; Lima, P.; Martins, I.C.; et al. A selective CuII complex with 4-fluorophenoxyacetic acid hydrazide and phenanthroline displays DNA-cleaving and pro-apoptotic properties in cancer cells. *Sci. Rep.* **2021**, *11*, 24450. [CrossRef]